Evidence for differential human slow-wave activity regulation across the brain

Zavada, Andrei; Strijkstra, Arjen M.; Boerema, Ate S.; Daan, Serge; Beersma, Domien G. M.

Published in:
Journal of Sleep Research

DOI:
10.1111/j.1365-2869.2008.00696.x

Publication date:
2009

doi: 10.1111/j.1365-2869.2008.00696.x

Evidence for differential human slow-wave activity regulation across the brain

ANDREI ZAVADA[1], ARJEN M. STRIJKSTRA[2], ATE S. BOEREMA[2], SERGE DAAN[2] and DOMIEN G. M. BEERSMA[2]

[1]Department of Informatics, Sussex University, Falmer, Brighton, UK and [2]Department of Chronobiology, University of Groningen, AA Haren, The Netherlands

Accepted in revised form 7 July 2008; received 10 August 2007

SUMMARY The regulation of the timing of sleep is thought to be linked to the temporal dynamics of slow-wave activity [SWA, electroencephalogram (EEG) spectral power in the ~0.75–4.5 Hz range] in the cortical non-rapid eye movement (NREM) sleep EEG. In the two-process model of sleep regulation, SWA was used as a direct indication of sleep debt, or Process S. Originally, estimation of the latter was performed in a gross way, by measuring average SWA across NREM–REM sleep cycles, fitting an exponential curve to the values thus obtained and estimating its time constant. In later studies, SWA was assumed to be proportional to the instantaneous decay rate of Process S, rather than taken as a direct reflection of *S*. Following up on this, we extended the existing model of SWA dynamics in which the effects of intrusions of REM sleep and wakefulness were incorporated. For each subject, a 'gain constant' can be estimated that quantifies the efficiency of SWA in dissipating *S*. As the course of SWA is variable across cortical locations, local differences are likely to exist in the rate of discharge of *S*, eventually leading to different levels of *S* in different cortical regions. In this study, we estimate the extent of local differences of SWA regulation on the basis of the extended model of SWA dynamics, for 26 locations on the scalp. We observed higher efficiency of SWA in dissipation of *S* in frontal EEG derivations, suggesting that SWA regulation has a clear local aspect. This result further suggests that the process involved in (local) SWA regulation cannot be identical to the Process S involved (with Process C) in effectual determination of sleep timing – a single behaviour that cannot vary between locations on the scalp. We therefore propose to distinguish these two representations and characterize the former, purely SWA-related, as 'Process Z', which then is different for different locations on the scalp. To demonstrate those differences, we compare the gain constants derived for the medial EEG derivations (Fz, Cz, Pz, Oz) with each other and with the decay rate derived from SWA values per NREM–REM sleep cycle.

KEYWORDS local SWA dynamics, sleep homeostasis, slow-wave activity, two-process model

INTRODUCTION

Sleep regulation research aims at the understanding of sleep behaviour and physiology. Even in the absence of full understanding of biochemical and neurophysiological functions of sleep, as well as of the underlying mechanisms, much is known about sleep homeostasis. In particular, studies of the dynamics of electroencephalogram (EEG) slow-wave activity (SWA, spectral EEG power in the delta frequency band) of non-rapid eye movement sleep (NREM sleep) have been successful in generating hypotheses concerning the regulatory mechanisms involved (Borbély, 1982; Daan and Beersma, 1983; Daan *et al.*, 1984; Dijk *et al.*, 1987; Dijk & Beersma, 1989; Dijk & Czeisler, 1995).

Correspondence: Dr Domien G. M. Beersma, Department of Chronobiology, University of Groningen, P.O. Box 14, 9750 AA Haren, The Netherlands. Tel.: +31 (0)50 363 2053; fax: +31 (0)50 363 2148; e-mail: d.g.m.beersma@rug.nl

The two-process model of sleep regulation (Borbély, 1982; Daan *et al*., 1984) is a widely accepted conceptual model of sleep timing. This model is based on two components: the homeostatic Process S, which increases during wakefulness and decreases in sleep, and a circadian Process C, which sets the upper and lower limits to Process S, under normally entrained conditions oscillating with a 24-h period. Sleep is initiated when the level of *S* reaches the upper threshold and terminated when it hits the lower threshold. The internal timing component, Process C, is independent of the homeostatic component, Process S (Daan *et al*., 1984). In the two-process model, dissipation of *S* during sleep follows an exponentially declining curve (towards $S = 0$). Similarly, an exponential increase towards an upper asymptote ($S = 1$) is assumed for the time course of *S* during wakefulness.

The time constant of the dissipation of *S* was originally derived by fitting an exponential curve to average SWA values per NREM–REM sleep cycle during sleep. The time constant of *S* build-up was estimated by fitting an exponential curve to the NREM sleep SWA data at the end and beginning of a baseline night and at the beginning of a recovery night after sleep deprivation (Daan *et al*., 1984). The rise rate has been validated by measuring NREM sleep EEG data in naps after varying durations of waking (Dijk *et al*., 1987; see, however, Werth *et al*., 1996).

In later studies, more attention has been paid to the detailed course of SWA. An extended model of SWA regulation was developed (Achermann *et al*., 1993). This model iteratively reconstructs the course of SWA of a night of sleep using a set of parameters, the hypnogram of the sleep episode, and the value of SWA at the beginning of it. The parameters define the rate of increase of SWA within NREM sleep bouts as well as the rate of SWA decrease due to intervening REM sleep and awakenings. It is further assumed that the instantaneous level of the need for SWA (as expressed in the value of *S*) limits the maximal possible actual amount of SWA. In turn, the actual amount of SWA will reduce the need for SWA. How much *S* is reduced per unit of SWA is expressed in a certain factor called the 'gain constant' (gc). This gain constant is thus a measure of efficiency with which SWA is dissipating *S*. Finally, it was shown by Achermann *et al*. (1993) that the assumption of a constant tendency for *S* to increase throughout all vigilance states (being overcompensated during sufficiently intensive NREM sleep) gives better simulations of the course of SWA. As a result, *S* can eventually increase during NREM sleep, as in NREM sleep stage 1 with sufficiently low levels of SWA. In accordance with the suggestion by Achermann *et al*., we have adopted this assumption in our simulations.

Process S plays a slightly different, though related role, in the two-process model (Daan *et al*., 1984) and in the SWA model of Achermann *et al*. (1993). It is primarily involved in the regulation of sleep timing in the two-process model, and it is primarily treated as a regulator of SWA in the SWA model. The characteristics of Process S required to obtain optimal simulations of the course of SWA (the SWA model) may not be identical to the characteristics required for the determination of sleep timing (the two-process model). An obvious problem is that SWA patterns in different areas of the cortex can be quite dissimilar, both at any given time (Cajochen *et al*., 1999) and along a stretch of time (Werth *et al*., 1997). To accommodate these dissimilarities, the *S* in the SWA-model (Achermann *et al*., 1993) must be made a local variable, while *S* in the two-process model (Daan *et al*., 1984) must remain a single parameter for the whole brain as long as the brain can be either asleep or awake.

In our study, we tested whether the simulations of SWA for different locations on the scalp require different courses of *S*. To avoid any confusion about the meaning of the processes we are interested in, we will distinguish these locally different instantiations of *S* from the original Process S involved in sleep timing, by the term 'Process Z'. In contrast to the single Process S, there may be multiple instantiations of Process Z, at different sites of the brain.

METHODS

Subjects and EEG data acquisition

Nine healthy young subjects (18–28 years) participated in an experiment using visual stimulation. Subjects did neither smoke nor use drugs, and abstained from consumption of alcohol and coffee throughout the experiment. They did not rate as extreme morning or evening types on the Horne–Östberg Morningness–Eveningness scale (Horne and Östberg, 1976), with mean ± SD at 46.7 ± 7.86. Six subjects were falling within the 'neither type' (range of neither type 42–58; entire range of scale: 16–86). Two subjects were moderately late (scores 34 and 39 respectively). One subject was moderately early (score 90). The experiment was approved by the Medical Ethics Committee of the Academic Hospital of the University of Groningen. Subjects signed an informed consent form.

Subjects were asked to come to the laboratory for a habituation sleep night and a baseline sleep night before a visual stimulation experiment took place on the third day. The results of the visual stimulation will be published elsewhere. For the present analysis, only the baseline sleep EEGs were used. Before both habituation and baseline sleep nights, subjects stayed at home doing their normal routine, until they came to the laboratory at 20:00 hours. After application of scalp electrodes (see below), subjects were asked to perform computerized test series of ~35-min duration starting at 22:00 hours and at 23:00 hours. The test series contained questionnaires and event related potential trials, and did not include other visual stimulation. Subjects prepared to go to sleep at 23:40 hours and went to bed and the electrodes were connected to the EEG amplifiers around 23:55 hours. At 00:00 hours, lights were turned off until 08:00 hours the next morning. Total time in bed was 8:04 ± 7 min (mean ± SD), sleep efficiency (time asleep to total time in bed) was 91.3 ± 2.7%, and NREM sleep latency (time from lights-out to the first occurrence of NREM sleep stage 2–4 of at least 1 min in length) was 14 ± 8 min.

Electroencephalograms were recorded using a cap system with Ag/AgCl electrodes (Electro-Cap International, Inc., Eaton, OH, USA), on 26 positions on the scalp (F7, F3, Fz, F4, F8, T3, C3, Cz, C4, T4, T5, P3, Pz, P4, T6, P9, P10, PO7, PO8, O1, Oz, O2, PO9, PO10, O9, O10). The left earlobe was initially used as reference, and the inion was used as ground. Data were amplified (500 μV/V) band-pass filtered between 0.16 and 30 Hz and sampled at 100 Hz. Besides EEGs, also electrooculogram of the right eye was obtained, and electromyogram was measured on neck muscles. EEGs were scored for wake, movement time, REM sleep and NREM sleep by 30-s epochs, using the criteria of Rechtschaffen and Kales (1968). For EEG recording and scoring, the EEG analysis program BrainVision (Brain Products, Gilching, Germany) was used. All EEG signals were re-referenced to the average signal of all derivations. Fast Fourier transformation with a Hanning window size of 3 s and 10% overlap was applied to produce power spectra for the 0–50 Hz range with 0.5 Hz resolution (by interpolation), for all 26 derivations. Only artefact-free portions of the EEG signal were included; artefact screening was performed by 3-s portions. Spectral power of all clean portions was then averaged over 30-s epochs.

The model

The modelling method follows the description of Achermann *et al*. (1993). Table 1 gives an overview of the parameters of the model. These parameters are used to compute, at 30-s intervals, the instantaneous rates of change of Z and SWA, from the initial value of SWA and the sequence of vigilance states. SWA fitting was performed between the simulated and empirical SWA profiles throughout the night using a least squares method, by iteratively adjusting parameters until the resulting improvement of the overall fit was considered sufficiently small ($< 0.05\%$). SWA simulations were performed for each 1-Hz bin in the 1–7 Hz range [i.e. a broader range than the conventional range of the δ-band (1 to ~4.5 Hz), for which there is extensive evidence of its homeostatic behaviour]. The fitting can fail if a parameter that theoretically is supposed to be positive goes to zero or to negative values during the fitting procedure. The equations are as follows:

$$dZ/dt = (-\mathrm{gc} \times \mathrm{SWA}) \times !\mathrm{WT} + (Z_U - Z) \times \mathrm{rs}, \quad (1)$$

$$\begin{aligned} d\mathrm{SWA}/dt = {} & \mathrm{rc} \times \mathrm{SWA} \times \mathrm{SWA} \times (Z/Z_U) \times (1 - \mathrm{SWA}/Z) \times !\mathrm{WT} \\ & - \mathrm{fc_R} \times (\mathrm{SWA} - \mathrm{SWA_L}) \times \mathrm{REMT} \\ & - \mathrm{fc_W} \times (\mathrm{SWA} - \mathrm{SWA_L}) \times \mathrm{WT}, \end{aligned} \quad (2)$$

where SWA and Z are current simulated values expressed as percentage of the mean SWA over all 30-s epochs scored as NREM sleep; $\mathrm{SWA_L}$ is the lower asymptote for SWA, defined as 95% of the lowest SWA observed in all 30-s REM sleep epochs; Z_U is the upper asymptote for Z; rc, gc, rs, $\mathrm{fc_R}$ and $\mathrm{fc_W}$ are sleep parameters described in Table 1. WT = 1 on wake, else 0; REMT = 1 during REM sleep, and also from t_a min before REM sleep, to allow for the SWA drop caused specifically by REM sleep, and for t_p min after completion of the REM sleep episode, because the effects of REM sleep interfering with SWA are still apparent for some time; t is time (in min). The operator '!' is logical negation (thus $!x = 0$ for any $x \neq 0$, and $!0 = 1$).

Table 1 Parameters of the model

Parameter	*Units*	*Description*	*Tunable*	*Initial value*
rc	$\mathrm{min^{-1}}$	SWA rise constant	Yes	0.283
$\mathrm{fc_R}$	$\mathrm{min^{-1}}$	SWA fall constant triggered by REM sleep	Yes	0.236
$\mathrm{fc_W}$	$\mathrm{min^{-1}}$	SWA fall constant triggered by wake	No	1
gc	$\mathrm{min^{-1}}$	Gain constant	Yes	0.835×10^{-2}
Z_0	%	Level of Z at sleep onset	Yes	300*
Z_U	%	Upper asymptote of Z	Yes†	400
t_a	min	Anticipated effect of REM sleep on SWA	No	6
t_p	min	Extension of effect of REM sleep on SWA	No	3
rs	$\mathrm{min^{-1}}$	Rise rate of Z	No	0.917×10^{-3}

Initial values derived by Achermann *et al*. (1993), representing the parameters for 'normal' sleep. The rise rate (rs) was derived from Daan *et al*. (1984).
*The 100% is defined, following Achermann *et al*. (1993), as the average SWA from the maximal common length of artefact-free 30-s intervals scored as NREM Stage 1–4. This length is 4 h 43 min.
†Z_U is tied to rs and not tuned independently:
$Z_U = (Z_0 - Z_{\mathrm{baseline\_end}} \times \exp(-t \times \mathrm{rs}))/(1 - \exp(-t \times \mathrm{rs}))$, t being here 24 h less the duration of the baseline night.

Our method of fitting the model equations comprises three nested loops, the innermost of which iterates along the timeline, per 30-s epoch (dt thus equals 30 s), to produce an SWA profile for a given set of parameter values. This is compared with the real SWA, and the quality of fit is calculated as a sum of squares of the differences between these in all SWA-containing 30-s epochs divided by the number of such epochs. At the end of the iteration, one of the tuneable parameters is given a fixed increment of random sign and the iteration is repeated. The fit is then compared to that from the previous run, and an increase or decrease in the deviation is used to retain or reverse the direction of the 'drift'; this is performed for each of the parameters, in random order. When a total of 400 iterations are completed, the resulting set of parameter values and the fit value are stored, again to be compared to the corresponding values from the previous iteration cycle (stride). Such strides, each resuming at parameter values where the preceding stride left off, are repeated until the improvement of the fit between two consecutive strides is $<0.05\%$ and no parameter has a drift on the last stride $>0.05\%$ of its initial value. Finally, the entire procedure, starting from randomization of initial parameters, was repeated four times and the best-fit outcome was chosen, thus helping minimize the probability of parameters settling in a local minimum. The described implementation was written in Octave (2.9 branch) and C++, and is available at http://chrono.biol.rug.nl/achermann.

The current experiment does solely include baseline sleep and no additional sleep episodes, which are needed to determine the rise rate of Process Z. The rise rate was therefore fixed at a value of 0.917×10^{-3} min^{-1}, which Daan *et al*. (1984) established for normal subjects in the experiments carried out by Borbély *et al*. (1981). This parameter defines the rate with which Z approaches its upper asymptote (Z_U) with time. As can be seen in Equation 1, Z is rising irrespective of vigilance state because $(Z_U - Z) \times \text{rs}$ is always positive. However, due to the term $(-\text{gc} \times \text{SWA})$, Z receives an additional decrement depending on the current value of SWA, such that it will decline during sufficiently intense NREM sleep. Likewise, in sufficiently shallow NREM sleep, Z will increase. This is where Achermann's concept of S, here termed Z, departs from the original definition of Process S in the two-process model of Daan *et al*. (1984): Achermann (followed by us here) allows the sleep debt to increase with longer but shallow sleep.

In the analyses presented below, only the gain constant is included. The other two parameters being estimated, SWA rise constant (rc) and SWA fall constant triggered by REM sleep (fc_R), were not found to have any systematic interdependencies, and are therefore kept constant.

Statistical comparisons of the gain constant scalp maps were performed using topographic ANOVA, or TANOVA, a Monte Carlo randomization non-parametric bootstrapping test used in EEG/EPR-related research [Manly (1991); Srebro (1996); Strik *et al*. (1998), the latter paper also contains a description of the TANOVA implementation used by us, which is slightly different from the one outlined by Srebro]. To visualize scalp maps of gc values (as well as to carry out TANOVA tests on scalp maps), data were processed in LORETA (vs. June 2003), an EEG/ERP/electromagnetic tomography program (Pascual-Marqui *et al*., 1994). To analyse differences in gc over an anterior to posterior cline on the scalp, repeated measures two-factor ANOVA with Holm–Sidak multiple comparisons of means was used (Sigmastat, San Jose, CA, USA).

RESULTS

Individual simulations

Figure 1 shows examples of the course of Z and simulated SWA superimposed on the measured SWA profile from the four medial derivations Fz, Cz, Pz and Oz in two subjects. Z has the same dimension as SWA (i.e. %) as in Achermann's

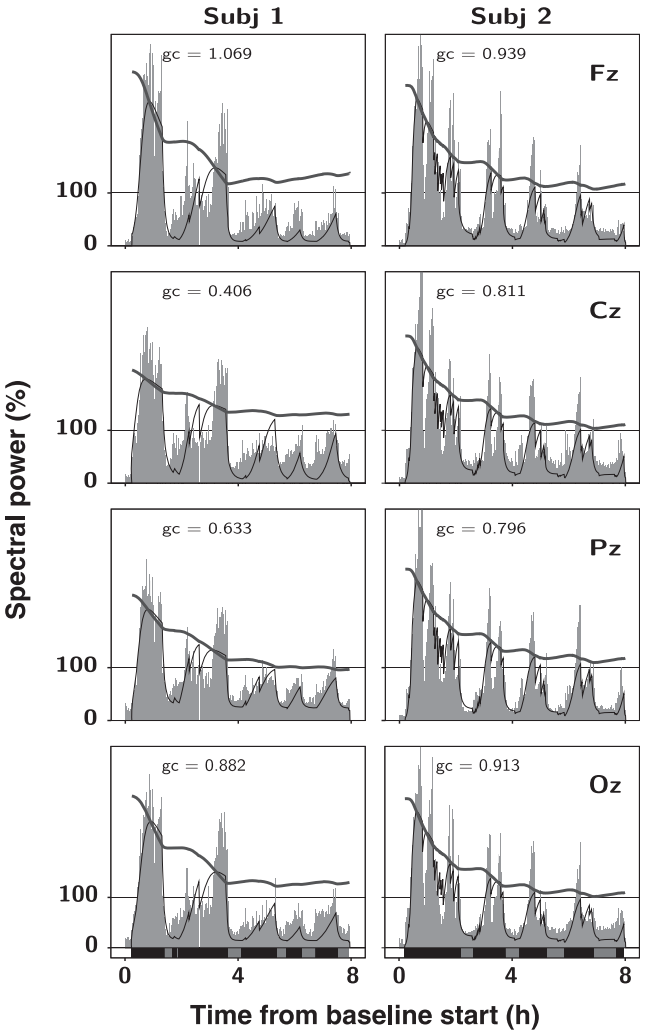

Figure 1. Simulation of SWA (thick black line) and Process Z (thin line) in the 2–3 Hz frequency range, plotted on top of the recorded SWA profile (solid grey area), in medial derivations obtained from two subjects. Z has the same dimension as SWA (i.e. %) as in Achermann's model. At the bottom of each panel, REM sleep is indicated as a half-height bar and NREM sleep as a full-height bar.

model. The original, dimensionless representation of Daan *et al*. (1984) becomes thus Z/Z_U. Both subjects showed a decrease in SWA over the sleep episode, albeit the shape of the SWA profile in Subject 1, with a wider trough between the first two most prominent SWA bouts, apparently posed a challenge to the simulation routine. It can be observed that the course of Z shows a rapid decrease during high SWA and a slower decrease or even increase during low SWA and REM sleep or wakefulness. Especially at the end of the sleeping episode, the rising Z demonstrates a behaviour by which it is distinct from a putative course of Process S reconstructed from the same empirical SWA.

By visual comparison, a gradual change across derivations in the relative amounts of SWA expressed in the first and next following NREM sleep bouts is already noticeable (Fig. 1). These changes are comprehensively given in the maps of Fig. 2.

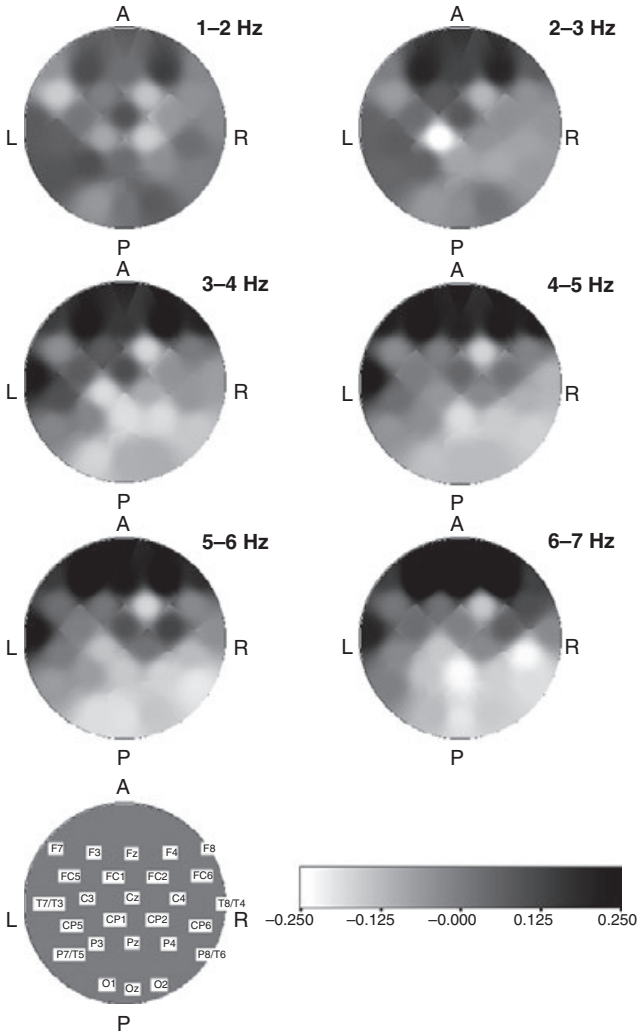

Figure 2. Distribution maps of the normalized average gain constant (gc) of all 26 derivations on the scalp (n = 6–9 per derivation). Normalization was performed by dividing each derivation gc value by the map average gc value. Scale bar indicates deviation of gc values from the average. The scalp is viewed from above, anterior side up.

It appears that larger reductions in the level of Z occur at Fz, as compared to the derivations posterior to it, which is demonstrated in Fig. 2 by larger gain constants in frontal over more occipital derivations. Of the 1404 possible 26 channels by six frequency bins by nine subjects combinations, EEG data were missing in 42 cases. Model failures occurred in 1.96% of the remaining 1362 simulation runs, most of them in subject 1, and these were due to either gc or fc_R approaching zero. The incidence of failures increased in higher frequency bins, reaching 8 in the 5–6 Hz bin, and 11 in the 6–7 Hz bin.

Gain constant maps

Figure 2 shows scalp maps of the normalized gc values from all 26 measured scalp locations, for all six 1-Hz intervals between 1 and 7 Hz. The common pattern is characterized by higher gc values in frontal areas. In a statistical analysis, gc in the 1–2 Hz map did not show significant deviation from the map average (P = 0.10). However, gain constant in the maps of the five higher 1-Hz frequency bins deviated significantly from the average map (TANOVA: $P < 0.05$). Table 2 summarizes the matrix of statistical assessment of differences between maps of different frequency bins of absolute gc values (in the lower-left triangle) and normalized gc value maps (in the upper-right triangle). For all but one map comparisons, differences in absolute gc value distributions were found, i.e. based on absolute differences and topographic differences combined. When absolute level effects were removed by normalization, the 1–2 Hz map still differed from all other maps. This indicates that gc behaves aberrantly in the 1–2 Hz, deviating from the distribution pattern with frontal high gc levels common to higher frequencies.

The gc maps suggest an anterior to posterior decline in gc values. To evaluate this, we analysed averaged gc values of frontal, central, parietal and occipital derivations around the midline (frontal: F3, Fz, F4; central: C3, Cz, C4; parietal: P3, Pz, P4; occipital: O1, Oz, O2) for changes with location, and the dependence of the change on the frequency bin. The normalized data of Fig. 2 were analysed with a two-factor repeated measures ANOVA with Holm–Sidak pair-wise multiple comparisons of means. Location had a significant effect ($F_{3,119}$ = 12.6, $P < 0.001$), with the highest gc values found at frontal locations, significantly higher than on all other locations ($P < 0.001$). Additionally, a significant interaction between location and frequency was found ($F_{15,119}$ = 3.7, $P < 0.001$), suggesting a frequency dependency of the gc cline. Location differences were not detected with Holm–Sidak comparisons of means within the 1–2 Hz frequency range, as could be expected by the absence of a significant map difference in that frequency range. Significant differences were found between locations in higher frequency bins: between the frontal and occipital locations for 2–3 Hz, between frontal and central/occipital locations for 3–4 Hz, between frontal and central/parietal/occipital locations for 4–5 Hz, between frontal and central/parietal/occipital locations and between parietal and occipital locations for 5–6 Hz, and finally, between

Table 2 Significance of differences between gc distribution maps between all 1-Hz frequency intervals overlapping with the delta range (topographic ANOVA, *significance at $P < 0.05$, **at $P < 0.01$)

Freq (Hz)	*1–2*	*2–3*	*3–4*	*4–5*	*5–6*	*6–7*
1–2	–	**	**	**	**	**
2–3	*	–	**	**	**	**
3–4	**	*	–	*	*	*
4–5	**	*	NS	–	NS	*
5–6	**	NS	NS	NS	–	*
6–7	**	**	**	*	*	–

NS, not significant.
Values in the upper right triangle: comparisons of absolute gc maps (indicating differences based on both gc level and gc map distribution); lower left triangle: within-map normalized values (indicating differences in gc map distribution only).

frontal and central/parietal/occipital locations and between central/parietal and occipital locations for 6–7 Hz. This indicates that an anterior to posterior cline indeed exists for gc values over the entire frequency range spanning the delta range, with the highest gc values at frontal locations. This cline appears to become more pronounced at higher frequency ranges.

Comparison of the gain constant and decay rate

We performed a decay rate estimation on a subset of our data, specifically on four medial EEG derivations, Fz, Cz, Pz and Oz. The estimation was performed by fitting an exponential curve of the form $SWA(t) = SWA_L + SWA_0 \exp(-r_d\ t)$, separately for the cases of $SWA_L = 0$ and $SWA_L \neq 0$, where SWA_L is the lower asymptote for SWA (% of night average), SWA_0 is the difference between its starting value and SWA_L (%), r_d is the decay rate (min^{-1}), and t is time (min). We also included, for comparison, a similar decay rate estimation by Mongrain *et al.* (2006), who let SWA_L be a free parameter. It must be noted, though, that Mongrain *et al.* used linked ear derivations as the reference signal, while we used the average of all derivations as a reference. Data points for the fitting were the average values of SWA expressed per single NREM–REM sleep cycle, and plotted at cycle midpoint. Each subject thus contributed several data points according to the number of NREM sleep bouts in their EEG profile. All group data were pooled and the fitting was performed.

The results are presented in Table 3. It can be observed that a non-zero SWA_L increases the quality of fit, while at the same time the antero-posteriorly decreasing trend in the decay rate, r_d, is no longer apparent.

DISCUSSION

In this study, we analysed the temporal patterns of SWA at multiple electrode positions by applying an elaborated version of Achermann's model of SWA regulation. The analysis was restricted to baseline sleep without sleep deprivation and thus was not aimed at a precise quantification of the rise rate of Process Z. Instead, we fixed the rise rate at the value Daan *et al.* (1984) established for normal subjects (0.917×10^{-3} min^{-1}). Dijk *et al.* (1987) observed on the basis of a nap-study that the rise rate of SWA across the day varies with the investigated frequency. The standard deviation of their data amounts to 20%. While their analysis is based on nap sleep data and on the first 30 min of NREM sleep per sleep episode, we prefer to use the estimated value of the rise rate of *S* from Daan *et al.* (1984) which is based on entire sleep nights without naps. To investigate the effect of fixing the rise rate, we performed additional estimations of gc using considerably higher (+30%: 1.200×10^{-3} min^{-1}) and lower (−30%: 0.600×10^{-3} min^{-1}) rise rates in the 2–3 Hz EEG frequency range data. These simulations resulted in small but similar gc changes in the all-derivations mean by +1.1% (0.649, SEM 0.016) for the high value, and −5.3% (0.608, SEM 0.015) for the low value, respectively, relative to the 'normal' condition gc value of 0.642, SEM 0.017 (all $\times 10^{-2}$ min^{-1}). Rise rate variation thus appears only marginally to affect the gain constant. We conclude that the fixing of the rise rate is not of significant importance for the interpretation of the present results.

Apart from fixing the rise rate to a constant value, our study is also limited by the fact that we analysed SWA regulation within 1-Hz frequency bins. The implicit assumption underlying this approach is that the regulation of Process Z in one 1-Hz bin is independent of its regulation in another 1-Hz frequency bin. While it is possible that the regulated processes are indeed confined to such specific frequency ranges, it is also conceivable that a single Process Z is modified by various NREM sleep EEG frequencies, in such a way that (for instance) long bouts of slow SWA modify *Z* also for its consequences on faster SWA. If that is the case, our assumption of independent regulation per 1-Hz frequency bin is not valid, and we should have analysed the regulation of *Z* for all relevant EEG frequencies simultaneously. For simplicity, we have not performed that. Instead, we have assumed that the 'cross-talk' between frequency bins is sufficiently limited to allow for independent analysis per 1-Hz frequency bin.

From the analysis of the gain constant in SWA regulation across multiple cortical locations, we find that the essential hourglass mechanism of dissipation of Process Z represented by gc is more clearly expressed in frontal areas. This is in accordance with Cajochen *et al.* (1999), who found a larger

Table 3 Simulation results for the derivations Fz, Pz and Oz (n = 9), Cz (n = 8), and a comparison of gain constant and decay rate, in the 2–3 Hz frequency range

Parameter	*Fz*	*Cz*	*Pz*	*Oz*
Achermann's method				
gc	0.795 ± 0.065	0.643 ± 0.052	0.608 ± 0.052	0.502 ± 0.086
rc	0.306 ± 0.032	0.280 ± 0.036	0.267 ± 0.030	0.215 ± 0.034
fc_R	0.167 ± 0.030	0.123 ± 0.029	0.146 ± 0.028	0.161 ± 0.033
Z_0	282.1 ± 13.4	259.9 ± 10.8	256.6 ± 10.8	249.4 ± 19.2
Z_U	394.0 ± 20.9	358.1 ± 18.6	347.6 ± 17.5	328.2 ± 31.8
fit	27.2 ± 2.9	26.4 ± 2.9	21.9 ± 2.4	27.0 ± 5.9
'Classic' estimation (with lower asymptote at 0): $SWA(t) = SWA_0 \exp(-r_d\, t)$				
SWA_0	165 ± 7	160 ± 8	151 ± 8	144 ± 10
r_d	0.189 ± 0.014	0.168 ± 0.015	0.150 ± 0.015	0.138 ± 0.020
R^2	0.86	0.81	0.76	0.61
'Classic' estimation (with a non-zero lower asymptote): $SWA(t) = SWA_L + SWA_0 \exp(-r_d\, t)$				
SWA_L	34 ± 11	50 ± 7	52 ± 8	33 ± 36
SWA_0	148 ± 10	144 ± 13	127 ± 13	118 ± 25
r_d	0.34 ± 0.08	0.45 ± 0.10	0.42 ± 0.12	0.23 ± 0.16
R^2	0.88	0.85	0.81	0.62
'Classic' estimation (with a non-zero asymptote) by Mongrain *et al.* (2006)				
r_d (morning types)	0.79 ± 0.14	0.85 ± 0.16	0.94 ± 0.18	1.09 ± 0.21
r_d (evening types)	0.46 ± 0.09	0.51 ± 0.10	0.55 ± 0.12	0.63 ± 0.14

For Mongrain *et al.*'s data (2006), n = 12, in each group contributing 62 (morning types) and 70 (evening types) data points for the fitting. Decay rate estimation was performed using the functions specified in the table. SWA levels, Z_0 and Z_U in % of mean in all valid 30-s epochs; r_d and gc in $min^{-1} \times 10^{-2}$, fc_R and rc in min^{-1}. The 'fit' for the Achermann's method results is a sum of squares of the differences between empirical and simulated courses of SWA in all SWA-containing 30-s epochs, expressed as percentage of the number of such epochs. Mean ± SEM. R^2 is the goodness-of-fit coefficient.

increase in frontal than in occipital SWA levels after sleep deprivation. In contrast, parieto-occipital areas appear to have lower gain constant, implying a smaller effect of local SWA on the decline of its regulating variable Z. The increased frequency of simulation failures in occipital areas suggests that Process Z has less explanatory power for the regulation of SWA at those locations. The observed local variation in the course of Process Z as a function of time and the differences in the Z level confirm our suspicion that Process Z is not identical across the cortex. As a consequence, Process S, supposed to control the timing of sleep, and Process Z, controlling SWA regulation, must be two different processes.

There is another argument consistent with our interpretation that S and Z are not exactly one and the same process. Achermann *et al.* (1993) have observed that SWA is simulated best under the assumption that Z always has a tendency to increase, only visible during sufficiently shallow NREM sleep. Such shallow NREM sleep often occurs in the later hours of the night, when sleep need is satiated. At this time, Z will effectively start increasing (as in Fig. 1, upper-left graph). Now, suppose Process Z is to interact with Process C to determine the time of awakening. The increasing Z in the later part of the night will approach the course of Process C at an acute angle, which will result in a relatively imprecise timing of sleep termination, considerably dependent on fluctuations in Z and C. Therefore, the functional suitability of Process Z in the regulation of sleep timing is limited, which fact furnishes an additional argument for the separation of the classical sleep need regulating Process S of the original two-process model from the purely SWA-related Process Z.

This conclusion cannot be definitive as long as we do not have direct assessments of the rise rates in wakefulness. Nonetheless, the clear differentiation of the gain constant over different cortical areas must mean that attributing a role in predicting sleep timing to SWA can only yield global predictions as there is no independent evidence for the specific involvement of particular cortical areas in the timing process. There are two speculative considerations that may salvage some of a brain-wide sleep-timing system. One is related to Process S, the other to Process C. (1) The recorded SWA constitutes just a glimpse of all electrical activity of the cells in the brain. It does not include those electrical activities that happen to cancel each other out. It also excludes all frequencies outside the SWA range. In addition, part of the electrical activity that is captured in SWA may not be directly involved in Process S. It is difficult to distinguish between S-related SWA and other SWA. As S-related SWA is expected to approach 0 after sufficient time spent in non-REM sleep, the

estimation of decay towards a non-zero asymptote can be observed as a modest attempt to distinguish between *S*-related (decaying) SWA and other SWA. The asymptotic value is conceived to allow for those non-*S*-related electrical activities. Indeed, with non-zero location-specific asymptotes, the decay rate of SWA appears to become rather constant over the investigated derivations (Table 3). If, after subtracting a location specific constant value from SWA, similar results could be obtained with the dynamic model defined by equations (1) and (2), this would suggest that there still is a single brain-wide Process S, with dynamics independent of location. Only it cannot be easily quantified on the basis of SWA because of the non-*S*-related processes. (2) From a functional point of view, one might expect that evolution has led to a system where each brain area carries out its repairs [whether these concern synaptic downscaling (Tononi and Cirelli, 2003), or other processes] simultaneously during the same behavioural sleep. If the rates of these processes are different in different areas, it would seem rather dysfunctional that the first area ready would trigger the end of sleep and prematurely wake up the whole rest of the brain. One might therefore expect that the local parameters of Process C (circadian clocks are ubiquitous in body and brain) would have coevolved and become adjusted to those of the local Process S. We will have to await the identification of the primary function of sleep and the direct assessment of its physiological correlates to establish firmly whether sleep regulation is indeed a whole brain process, or has local, distinct peculiarities. Until that time, it seems appropriate to distinguish clearly local SWA regulation (*Z*) from global *S* regulation.

ACKNOWLEDGEMENTS

The work was supported by NWO (PVA) grant 580-02.102 (Circadian and behavioural determinants of fatigue) to D. G. M. Beersma and S. Daan. A. Zavada received scholarship as an Ubbo Emmius bursary at the University of Groningen, the Netherlands. Our work is further supported by the EC 5th framework program BrainTime (QLG3-CT-2002-01829) and the 6th Framework Integrated Program EUCLOCK (018741). We thank Dr A. A. Wijers for expert help with the use of the multielectrode cap.

REFERENCES

Achermann, P., Dijk, D.-J., Brunner, D. P. and Borbély, A. A. A model of human sleep homeostasis based on EEG slow-wave activity: quantitative comparison of data and simulations. *Brain Res. Bull.*, 1993, 31: 97–113.

Borbély, A. A. A two process model of sleep regulation. *Hum. Neurobiol.*, 1982, 1: 195–204.

Borbély, A. A., Baumann, F., Brandeis, D., Strauch, I. and Lehrmann, D. Sleep deprivation: effect on sleep stages and EEG power density in man. *Electroencephalogr. Clin. Neurophysiol.*, 1981, 51: 483–493.

Cajochen, C., Foy, R. and Dijk, D.-J. Frontal predominance of a relative increase in sleep delta and theta EEG activity after sleep loss in humans. *Sleep Res. Online*, 1999, 2: 65–69.

Daan, S. and Beersma, D. G. M. Circadian gating of human sleep–wake cycles. In: M. C. Moore-Ede and C. A. Czeisler (Eds) *Mathematical Models of the Circadian Sleep–Wake Cycle*. Raven Press, New York, 1983: 129–158.

Daan, S., Beersma, D. G. M. and Borbély, A. A. Timing of human sleep: recovery process gated by a circadian pacemaker. *Am. J. Physiol.*, 1984, 246: R161–R178.

Dijk, D.-J. and Beersma, D. G. M. Effects of SWS deprivation on subsequent EEG power density and spontaneous sleep duration. *Electroencephalogr. Clin. Neurophysiol.*, 1989, 72: 312–320.

Dijk, D.-J., Beersma, D. G. M. and Daan, S. EEG power density during nap sleep: reflection of an hourglass measuring the duration of prior wakefulness. *J. Biol. Rhythms*, 1987, 2: 207–219.

Dijk, D.-J. and Czeisler, C. A. Contribution of the circadian pacemaker and the sleep homeostat to sleep propensity, sleep structure, electroencephalographic slow waves, and sleep spindle activity in humans. *J. Neurosci.*, 1995, 15: 3526–3538.

Horne, J. A. and Östberg, O. A self-assessment questionnaire to determine morningness-eveningness in human circadian rhythms. *Int. J. Chronobiol.*, 1976, 4: 97–110.

Manly, B. F. J. *Randomization and Monte Carlo Methods in Biology*. Chapmann and Hall, London, 1991.

Mongrain, V., Carrier, J. and Dumont, M. Difference in sleep regulation between morning and evening circadian types as indexed by antero-posterior analyses of the sleep EEG. *Eur. J. Neurosci.*, 2006, 23: 497–504.

Pascual-Marqui, R. D., Michel, C. M. and Lehmann, D. Low resolution electromagnetic tomography: a new method for localizing electrical activity in the brain. *Int. J. Psychophysiol.*, 1994, 18: 49–65.

Rechtschaffen, A. and Kales, A. A. *A Manual of Standardized Terminology, Techniques and Scoring System for Sleep Stages of Human Subjects*. U.S. Department of Health, Education, and Welfare, Bethesda, 1968.

Srebro, R. A bootstrap method to compare the shapes of two scalp fields. *Electroencephalogr. Clin. Neurophysiol.*, 1996, 100: 25–32.

Strik, W. K., Fallgatter, A. J., Brandeis, D. and Pascual-Marqui, R. D. Three-dimensional tomography of event-related potentials during response inhibition: evidence for phasic frontal lobe activation. *Electroencephalogr. Clin. Neurophysiol.*, 1998, 108: 406–413.

Tononi, G. and Cirelli, C. Sleep and synaptic homeostasis: a hypothesis. *Brain Res. Bull.*, 2003, 62: 143–150.

Werth, E., Dijk, D.-J., Achermann, P. and Borbély, A. A. Dynamics of the sleep EEG after an early evening nap: experimental data and simulations. *Am. J. Physiol.*, 1996, 271: R501–R510.

Werth, E., Achermann, P. and Borbély, A. A. Fronto-occipital EEG power gradients in human sleep. *J. Sleep Res.*, 1997, 6: 102–112.